The Meteoritical Society

Meteoritics & Planetary Science 47, Nr 9, 1436–1448 (2012)
doi: 10.1111/j.1945-5100.2012.01406.x

The isotopic composition and fluence of solar-wind nitrogen in a genesis B/C array collector

Gary R. HUSS[1*], Kazuhide NAGASHIMA[1], Amy J. G. JUREWICZ[2], Donald S. BURNETT[3], and Chad T. OLINGER[4]

[1]Hawai'i Institute of Geophysics and Planetology, University of Hawai'i at Mānoa, 1680 East-West Road, POST 504, Honolulu, Hawai'i 96822, USA
[2]Center for Meteorite Studies, Arizona State University, 550 East Tyler Mall, PSF-686, Tempe, Arizona 85287–1404, USA
[3]Division of Geological and Planetary Science, California Institute of Technology, Mail Code 100-23, 1200 E. California Blvd., Pasadena, California 91125, USA
[4]Applied Modern Physics, Los Alamos National Laboratory (MS D434), Los Alamos, New Mexico 98544, USA
[*]Corresponding author. E-mail: ghuss@higp.hawaii.edu

(Received 06 April 2011; revision accepted 22 July 2012)

Abstract–We have measured the isotopic composition and fluence of solar-wind nitrogen in a diamond-like-carbon collector from the Genesis B/C array. The B and C collector arrays on the Genesis spacecraft passively collected bulk solar wind for the entire collection period, and there is no need to correct data for instrumental fractionation during collection, unlike data from the Genesis "Concentrator." This work validates isotopic measurements from the concentrator by Marty et al. (2010, 2011); nitrogen in the solar wind is depleted in ^{15}N relative to nitrogen in the Earth's atmosphere. Specifically, our array data yield values for $^{15}N/^{14}N$ of $(2.17 \pm 0.37) \times 10^{-3}$ and $(2.12 \pm 0.34) \times 10^{-3}$, depending on data-reduction technique. This result contradicts preliminary results reported for previous measurements on B/C array materials by Pepin et al. (2009), so the discrepancy between Marty et al. (2010, 2011) and Pepin et al. (2009) was not due to fractionation of solar wind by the concentrator. Our measured value of $^{15}N/^{14}N$ in the solar wind shows that the Sun, and by extension the solar nebula, lie at the low-$^{15}N/^{14}N$ end of the range of nitrogen isotopic compositions observed in the solar system. A global process (or combination of processes) must have operated in interstellar space and/or during the earliest stages of solar system formation to increase the $^{15}N/^{14}N$ ratio of the solar system solids. We also report a preliminary Genesis solar-wind nitrogen fluence of $(2.57 \pm 0.42) \times 10^{12}$ cm^{-2}. This value is higher than that derived by backside profiling of a Genesis silicon collector (Heber et al. 2011a).

INTRODUCTION

Importance of Nitrogen to Planetary Materials

Nitrogen is the fifth most abundant element in the solar system. The $^{15}N/^{14}N$ ratio varies dramatically among solar system objects, from approximately 2.3×10^{-3} in Jupiter (Owen et al. 2001) and in osbornite (TiN) in a refractory inclusion from a CH chondrite thought to be among the earliest-formed solids (Meibom et al. 2007), to approximately 3.7×10^{-3} in the atmospheres of Earth and Venus and in Martian rocks, to $6–7 \times 10^{-3}$ in CN and HCN molecules in the comas of comets (Bockelée-Morvan et al. 2008), to values as high as approximately 8×10^{-3} in some dark inclusions from CH and CB chondrites (e.g., Bonal et al. 2010). The nitrogen isotopic composition of the Sun is a key constraint for understanding the origin of the isotopic variations in nitrogen because the Sun contains approximately 99.8% of the mass of the solar system and thus is representative of the nitrogen composition of the bulk solar system.

Historically, scientists attempted to determine the nitrogen isotopic composition of the Sun from solar wind trapped in lunar soils. Results seemed to indicate that soils exposed long ago (1–3 Ga) were depleted in

^{15}N by approximately 20% relative to the Earth's atmosphere. In contrast, soils exposed during the last 200 million years show ^{15}N enrichments (Kerridge 1993; Kim et al. 1995). Observations such as these led to the hypothesis of a secular variation in the nitrogen isotopic composition of the solar wind (e.g., Kerridge 1993), but this hypothesis is hard to reconcile with astrophysics (Geiss and Bochsler 1982, 1991). Alternatively, these variations may indicate mixing of various lunar, cometary, or asteroidal reservoirs with the solar wind (e.g., Geiss and Bochsler 1982, 1991; Wieler et al. 1999; Hashizume et al. 2000).

Importance of Nitrogen to Solar Physics

The solar physics community is interested in obtaining precise fluences and isotopic compositions in order to fully understand the mechanisms that ionize and accelerate the atoms comprising the solar wind. Solar wind is fractionated relative to the photosphere. Elements with a low first ionization potential (FIP), < 10 eV such as magnesium, silicon, and iron, are enriched relative to oxygen in the solar wind compared with the photosphere, with the largest enrichments observed in the slow solar wind (e.g., von Steiger et al. 2000). Because elemental fractionation in the solar wind can be thought of as the result of a competition between photoionization and dynamic atom-ion separation, Geiss et al. (1994) proposed that a model based on the first ionization time (FIT) provides a better description of the fractionation in solar wind. FIP and FIT affect the pool of ions from which some portion is accelerated to form the solar wind. They predict different solar wind elemental fractionations, and are not expected to produce isotopic fractionations. Inefficient coulomb drag (ICD) during the acceleration of the solar wind is also capable of producing fractionations (e.g., Bodmer and Bochsler 2000; Bochsler 2007). This process can fractionate isotopes as well as elements because coulomb drag depends in part on the masses of the interacting particles. Nitrogen is a key element for evaluating these various models.

Role of the Genesis Mission

NASA's Genesis Mission was designed to capture contemporary solar wind under clean conditions and return it to Earth for analysis. The nitrogen isotopic composition of the solar wind was one of the highest priority objectives of the Genesis mission (e.g., Burnett et al. 2003). Several research groups have attempted to measure the nitrogen isotopic composition of the solar wind. The CNRS group at Nancy, France, measured the gold-plated arms of the cross that provided the frame for the targets in the electrostatic concentrator (Marty et al. 2010). Nitrogen and noble gases were extracted using a 193 nm UV laser defocused to approximately 50×150 μm and, after purification, were measured in a static mass spectrometer. Extraction efficiency was high, but the solar-wind nitrogen was contaminated by large amounts of terrestrial nitrogen, resulting in a low signal-to-noise ratio. From multiple measurements, and using the measured $^{20}Ne/^{14}N$ ratios normalized to the ratio in the solar wind to infer the fraction of solar-wind nitrogen in each measurement, Marty et al. (2010) derived a best estimate of $(^{15}N/^{14}N)_{sw} = (2.26 \pm 0.67) \times 10^{-3}$ (2σ). On the basis of these data, one would conclude that, relative to Earth's atmosphere, the solar wind is depleted in ^{15}N by approximately 40% ($\delta^{15}N = -385 \pm 182‰$).

Another group at the University of Minnesota measured nitrogen from collector material consisting of a thin film of gold deposited on sapphire (AuOS) from the B/C bulk solar wind collector (Pepin et al. 2009; Becker 2010). The nitrogen was released from the gold in the collector by room temperature amalgamation with mercury, which discriminates against nitrogen contained in organic contaminants. The released nitrogen was cleaned up and measured by static mass spectrometry. The measured nitrogen is estimated to consist of 15–80% solar-wind nitrogen. Although the level of contamination is probably low, the yield of solar-wind nitrogen is also low in these experiments, with the largest yield estimated at approximately 50%. The resulting estimate of the $(^{15}N/^{14}N)_{sw}$ is approximately 4.9×10^{-3} ($\delta^{15}N = \sim +325‰$) (Pepin et al. 2009).

The results of these two studies could not be more different, with one group reporting approximately 40% depletion of ^{15}N and the other reporting approximately 30% excess of ^{15}N. To address this discrepancy, a third study was carried out on the Genesis solar wind concentrator silicon carbide target #60001 using the UCLA MegaSIMS (Kallio et al. 2010). Five depth profiles were measured at two different radii on the collector (approximately 10 mm and approximately 21 mm). Preliminary results from this study give $(^{15}N/^{14}N)_{sw}$ = approximately $(1.85–2.05) \times 10^{-3}$ ($\delta^{15}N$ = approximately -440 to $-495‰$). These results support the result from Marty et al. (2010). Most recently, Marty et al. (2011) used the Cameca ims 1280HR2 at CRPG-CNRS Nancy, France to measure the #60001 SiC concentrator target. Using these new data, they have refined their estimate of the solar wind composition to $(2.18 \pm 0.02) \times 10^{-3}$ ($-407 \pm 7‰$, 2σ), from which they derive a composition for the Sun of $(2.27 \pm 0.03) \times 10^{-3}$ ($-382 \pm 8‰$).

A potential problem with measurements of the concentrator target or the gold cross is that the

concentrator introduces a significant mass-dependent fractionation of the solar wind (Wiens et al. 2003; Marty et al. 2010; McKeegan et al. 2010). An instrumental mass fractionation curve for Ne in the #60001 target measured by Heber et al. (2011b) has been used as a basis for handling instrumental mass fractionation. However, to remove any ambiguity between data from concentrator versus array collectors, as well as to address the difference between the results of the Nancy and University of Minnesota laboratories, the Mission PI and University of Hawai'i ion microprobe group decided to measure the nitrogen isotopic abundances in a Genesis diamond-like carbon on silicon (DOS) collector from the B/C bulk solar wind array using the Cameca ims 1280 housed in the W. M. Keck Cosmochemistry Laboratory at the University of Hawai'i. Although the amount of solar-wind nitrogen per unit area in the arrays is significantly lower than in the concentrator targets, enough nitrogen was present for a measurement of both isotopic composition and fluence. This paper reports the results of our measurements.

EXPERIMENTAL METHODS

The nitrogen measurements made by Marty et al. (2011) used a concentrator SiC collector, which had a very low nitrogen blank. Unfortunately, there was no SiC in the BC array. The collector material selected for this experiment was diamond-like carbon on silicon (DOS). This material was used both in the concentrator and in the bulk solar wind array. The diamond-like carbon is a relatively thick (about 1 μm), semi-ordered film on a silicon substrate that was made for Genesis by Sandia National Laboratories. The concentrator target was intended for nitrogen measurements, and it was verified to have a low nitrogen background in the surface layers (Jurewicz et al. 2003). The B/C array DOS collector was not intended for measuring nitrogen. During its manufacture, there was an annealing step that can potentially result in atmospheric contamination in the top 200 nm. The amount of this contamination was expected to be about 20% of the unconcentrated solar wind abundance, but because it appeared to be homogeneously distributed, Jurewicz et al. (2003) stated that nitrogen measurements might be possible in this material. Although not ideal, the DOS collectors in the bulk solar wind B/C array are the only samples suitable for this experiment.

The sample used for this work was #60628 from the Genesis B/C array. This piece is approximately 6 × 6 mm in size. The sample was cleaned at JSC using their standard protocol. The surface has minor damage in places and there were still several particles on the surface. For measurements, we selected undamaged areas that had no visible particles.

Solar wind ions are implanted at depth in the collector, with solar-wind nitrogen peaking approximately 25 nm below the surface of the diamond-like carbon array collector. Because the solar wind is a constant velocity plasma, ^{15}N will be implanted deeper than ^{14}N. Accordingly, measurement protocols and subsequent data reduction must resolve the solar wind signal as a function of depth in the collector. Therefore, depth profiles were collected using a rastered Cs^+ primary beam and the final depth of each pit was measured.

The profiles were quantified using a laboratory implant of known fluence in the same type of collector material: here, a H-^{18}O-^{15}N implant into a flight-like sample of DOS manufactured at Sandia National Laboratory. Nitrogen-15 was implanted by Leonard Kroko, Inc. at a level of 1×10^{15} cm^{-2} at 45 keV, an energy that is approximately 3 times higher than the energy of the solar wind. Using deeper implants reduces the effects of surface contamination of the standard calibration (see below). Hydrogen was implanted later at Los Alamos National Laboratory at 1.8×10^{16} cm^{-2} at 10 keV (approximately 10 times higher energy than the solar wind) to simulate the hydrogen dose from the solar wind. A depth profile through the standard implant is shown in Fig. 1.

No correction was made for instrumental mass fractionation of the nitrogen isotopes in the ion probe because we do not have suitable standards and because previous experience has shown that nitrogen isotopic fractionation is less than approximately 30‰. The systematic uncertainty from not correcting for mass fractionation is a small part of the total uncertainty and does not affect the results of this work.

Details of the measurement protocol and data reduction are discussed below.

Measurement Protocol

Because of the small concentration of nitrogen in the array collectors, instrumental background is a problem for measurements of nitrogen isotopes. Accordingly, we did several things to reduce the background gas in the instrument. First, we mounted Genesis B/C array sample #60628 along with our ^{15}N reference implant and a silicon wafer in the same sample holder, which was placed into the airlock (approximately 10^{-8} torr) for three days before the measurement was to begin. Concurrently, our Ti sublimation pump was used to reduce the background in the sample chamber itself. The night before the measurements were to start, we moved the sample holder to the sample chamber and used a 20 nA Cs^+ beam to raster a 500 × 500 μm square on the silicon wafer for 14 h. Sputtered silicon ions act as a getter to gaseous oxygen, carbon, and perhaps nitrogen,

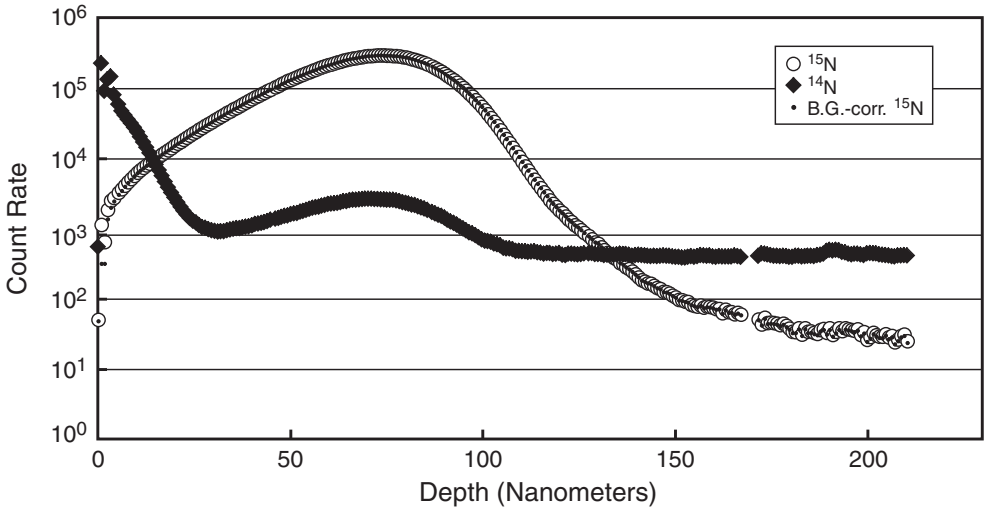

Fig. 1. Standard implant profile for ^{15}N into flight-like diamond-like carbon on silicon (DOS). The implant dose of ^{15}N was 1×10^{15} cm^{-2}, implanted at 45 keV. The ^{14}N signal is a combination of surface contamination gardened into the DOS, a small amount of implanted ^{14}N (the bump that occurs at the same depth as ^{15}N), and background nitrogen in the DOS collector material. Background ^{15}N, roughly a part in 10^4 of the peak, can be estimated by dividing the ^{14}N count rate by 272 (the terrestrial $^{14}N/^{15}N$ ratio). The background-corrected ^{15}N profile is shown by the small dots that overlay to measured ^{15}N profile.

further reducing residual gases in the sample chamber. Following these procedures, the vacuum in the sample chamber was approximately 6.3×10^{-10} torr. A liquid nitrogen trap further reduced the pressure in the sample chamber during the analytical session ($2–3 \times 10^{-10}$ torr).

Nitrogen isotopes were measured as CN^- using a Cs^+ primary ion beam that impacted the sample with an energy of 20 keV. The required mass resolving power (MRP) is approximately 7500, but before measurements were made, we scanned the CN^- peaks on the ^{15}N implant at a MRP of 11,500 to make sure that there were no interferences that we did not anticipate. Measurements were carried out by depth profiling using a 50×50 μm^2 raster. A focused primary ion beam of 0.75 nA was used and a measurement consisted of 300 cycles of mass 26 ($^{12}C^{14}N$) for one second and mass 27 ($^{12}C^{15}N$) for ten seconds. Data were collected using the monocollector electron multiplier.

To minimize the contribution of residual gaseous nitrogen from the sample chamber, we used a field aperture in combination with the dynamic transfer optical system (DTOS). The field aperture was set to mask all but a 37×37 μm^2 area on the sample (3000 micron field aperture and transfer magnification setting of approximately 100), while the DTOS deflects the ions sputtered by the primary-ion-beam so that they appear in the center of the field aperture. Ions generated in the gas above the sample do not correlate with the position of the primary ion beam, and thus are not centered by the DTOS. The combination of relatively small field aperture and DTOS cuts the background significantly. To further reduce the contribution of unwanted nitrogen to our signal, we used the electronic gate to exclude the ions from the outer 50% of the sputtered area, thus eliminating contributions from the crater walls and from nitrogen creeping along the surface of the collector.

We tried to degas the surface of the sample prior to the measurement using the electron gun with 20 eV of energy, as we have done for hydrogen, but this did not reduce the surface contamination significantly. The surface-contamination nitrogen appears to be tightly bound. Sputtering of this surface layer with the primary beam used for the depth profile generated a large "knock-on" background that persisted well into the expected depth of the solar-wind implant. The final measurement protocol used low energy (approximately 7 keV impact energy) primary ions to presputter the sample surface (Mao et al. 2008). This was much more effective at removing contaminant nitrogen close to the surface, significantly reducing "knock-on" contamination deeper in the sample. For the measurement reported here, the sample surface was presputtered with a 0.5 nA primary ion beam at 7 keV for 60 min (points 1 and 2) and for 15 min (points 3–11). The presputtered region was approximately 250×250 μm^2, sufficient to remove the surface layer for some distance around the measurement crater. Depths of presputter craters are estimated to be approximately 5 nm for the 60-min presputter and approximately 1 nm for the 15-min presputter. Although this presputtering did not completely eliminate "knock-on" nitrogen, it did significantly reduce the background from this source.

Even with all of these procedures in place, the initial signal was overwhelmingly dominated by surface

nitrogen. Surface-correlated background, including the knock-on nitrogen, declined approximately exponentially with time or depth. The surface nitrogen asymptotically approached the steady-state intrinsic background associated with the diamond-on-silicon collector material, reaching a plateau at approximately 40 nm depth, as determined by subtracting a model solar wind implant (see below). This background signal from the collector material was approximately 500 cps. In comparison, the implant signal peaks at approximately 650 cps.

Crater depths were measured using an Alpha Step 200 profilometer at Arizona State University. The accuracy of this instrument using our procedure has been tested recently by comparing pit depths measured at ASU with those measured on the same samples by an independent instrument, located at NIST. The average pit-depth difference was less than 1% for pits similar to those measured here.

Data Reduction

The first step in the data reduction was to apply the appropriate deadtime correction. The measured count rate was first corrected for the fraction of the time that the beam did not go into the electron multiplier due to the E-gate (in this case, 50% of the time), and then the count rate was corrected for the multiplier deadtime of 31 ns. Then, because the two isotopes were measured sequentially, not simultaneously, the signals had to be time interpolated to correct for the time-dependent variations in the ion-signal strength. The profiles must also be converted to depth profiles. This was done using a sputtering rate calculated from the total depth of the crater minus the depth of the presputtering crater (estimated based on the presputter beam current and raster size because the crater was too shallow to measure directly) and scaling to the beam current. Although the treatment of the presputter craters is not ideal, they are shallow enough (1–5 nm) that an uncertainty of a factor of two is not enough to change the results. The data were then corrected for various types of nitrogen not of solar-wind origin, and the $^{15}N/^{14}N$ for the solar wind was calculated. Two different methods of data reduction were carried out independently by two of the authors (GRH and DSB), both comparing data with simulations of the implant process. The simulations will be detailed below, followed by discussions of the data reduction methods.

Simulations

Simulations used the open source code: stopping and range of ions in matter (SRIM) (Ziegler 2004; Ziegler et al. 2010). Input files of 1,000,000 ions representing solar-wind nitrogen were generated using a Monte Carlo routine that uses the average of the carbon and oxygen flux distribution as a function of wind speed as measured by the ACE spacecraft. These were set at normal incidence into a carbon target with density of 2.85 g cm^{-3}. Ion ranges in the carbon were collected in SRIM and postprocessed to establish range distributions for each isotope (Fig. 2).

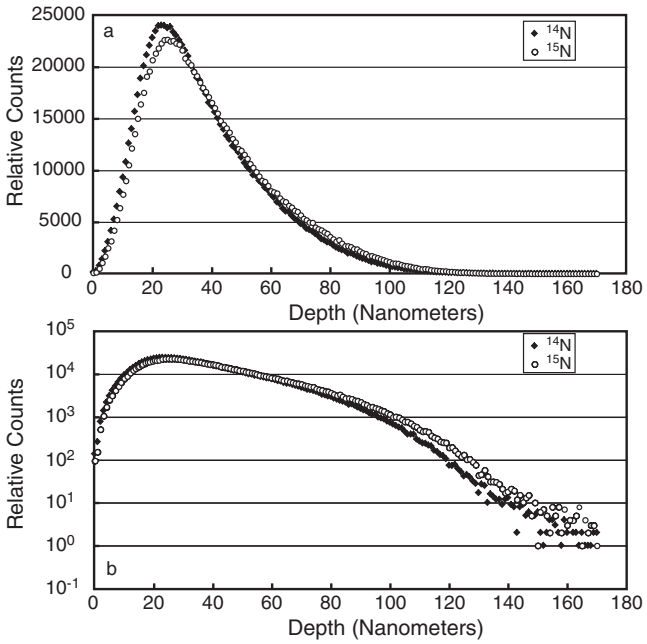

Fig. 2. Simulated implant profiles for ^{14}N and ^{15}N in diamond-like carbon (density = 2.85 g cm^{-3}) calculated using the SRIM program for the average of the carbon and oxygen flux distributions as a function of wind speed for the bulk-solar-wind velocity distribution. Panel "a" shows the profiles on a linear scale, while panel "b" shows the same profiles on a log scale. Note that the ^{15}N profile is offset to a greater depth compared with the ^{14}N profile, as expected due to its lower momentum-transfer rate to diamond.

Determination of the $^{15}N/^{14}N$ Ratio in the Solar Wind

Method 1

For this method, the measured ^{14}N and ^{15}N profiles were corrected for the background nitrogen in the collector using the ^{14}N signal and average $^{15}N/^{14}N$ ratio from below the level of the implant (> 100 nm). A SRIM-calculated solar-wind profile for ^{14}N was scaled to match the measured ^{14}N profile in the region from approximately 30 to 100 nm (Fig. 3). The match is very good, showing that the background-corrected measurement is dominated by solar-wind nitrogen in that region. This allows us to use the background-corrected profiles as direct measures of the solar-wind nitrogen. The portion of the measured, background-corrected ^{14}N and ^{15}N profiles between 30 and 90 nm were integrated

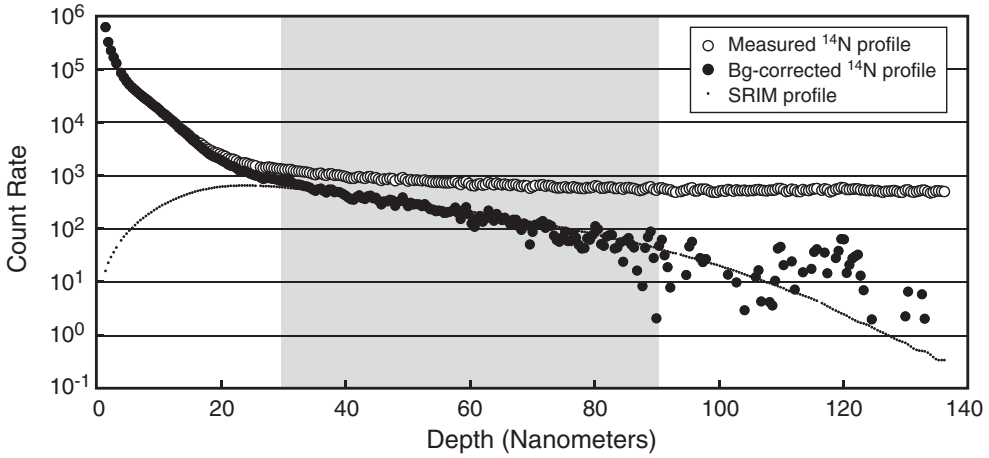

Fig. 3. This figure compares the measured ^{14}N profile in the B/C array (open symbols) with the same profile corrected for the intrinsic background in the collector material (solid symbols) and with the SRIM implant profile for solar-wind nitrogen, scaled to facilitate comparison (dots). In data-reduction Method 1, the portion of the background-corrected profile between 30 and 90 nm (shaded region) was used to calculate the nitrogen isotopic composition in the solar wind.

and the resulting values were used to calculate the $^{15}N/^{14}N$ ratio for each measurement.

Method 2

In this method, the SRIM profile of solar wind ^{14}N implanted into diamond-like carbon (Fig. 2) was assumed to accurately model the nitrogen profile in the Genesis collector. The SRIM profile and the measured sample profiles are all discrete digital profiles, but the depth scales differ (even though all give absolute depths). To use the SRIM profile directly to reduce the measurement data, the depth scale had to be converted to match the depths for each measurement cycle. This was done using a cubic spline interpolation of the calculated SRIM profile after applying a smoothing function (5-point running average).

The cubic-spline-adjusted profile was assumed to represent the solar wind profile in the Genesis collector, but it had to be normalized correctly. This was done by subtracting different amounts of the SRIM profile for ^{14}N from each measured ^{14}N profile until the resulting profile was flat for depths greater than approximately 40 nm (Fig. 4). The remaining part of the measured profile was assumed to represent the background for ^{14}N in each measurement. The scaled SRIM profile for each measurement was assumed to represent the solar wind ^{14}N profile. For all measured profiles, the inferred amount of solar wind subtracted was almost the same (fortunately), but each profile was calculated separately. We did not use an "average" SRIM profile on all measurements. The $^{15}N/^{14}N$ ratio of the background was determined by averaging the results from the first 10 cycles and last 50 cycles of each measurement. The background ^{15}N profile was calculated from this ratio and the ^{14}N background profile. The background ^{15}N profile was then subtracted from the measured ^{15}N profile to give the solar wind ^{15}N profile. The scaled SRIM profile for ^{14}N and the background-corrected ^{15}N profile were then integrated separately from 20 to 85 nm and the final ratio was calculated for each measurement.

We tried a third method in which we attempted to correct for the surface contamination by fitting the background with an appropriate curve and then subtracting this background and the deep background from the measured profile. However, we were not able to obtain satisfactory fits to the shallow background, and we could not reliably extract a plausible solar wind profile using this method.

SRIM modeling indicates that the peak of the ^{15}N solar wind implant is approximately 2 nm deeper than the peak of the ^{14}N implant, and the tail of the ^{15}N implant is also substantially deeper (Fig. 2). Because we do not integrate the entire implant to determine the $^{15}N/^{14}N$ ratio, a correction is required for this depth offset. Our data are not precise enough to resolve this offset well enough to account for it based on the measurements alone. Therefore, we used the SRIM profiles to estimate the bias introduced by calculating the nitrogen isotope ratio from slightly different portions of the ^{14}N and ^{15}N profiles. The factors used to correct $\delta^{15}N$ are approximately –67‰ for Method 1 and –32‰ for Method 2. These corrections have been applied to the data in Table 1.

Uncertainties

The two-sigma statistical uncertainty of an individual ratio measurement using either Method 1 or Method 2 is on the order of ±25%. This is similar to the

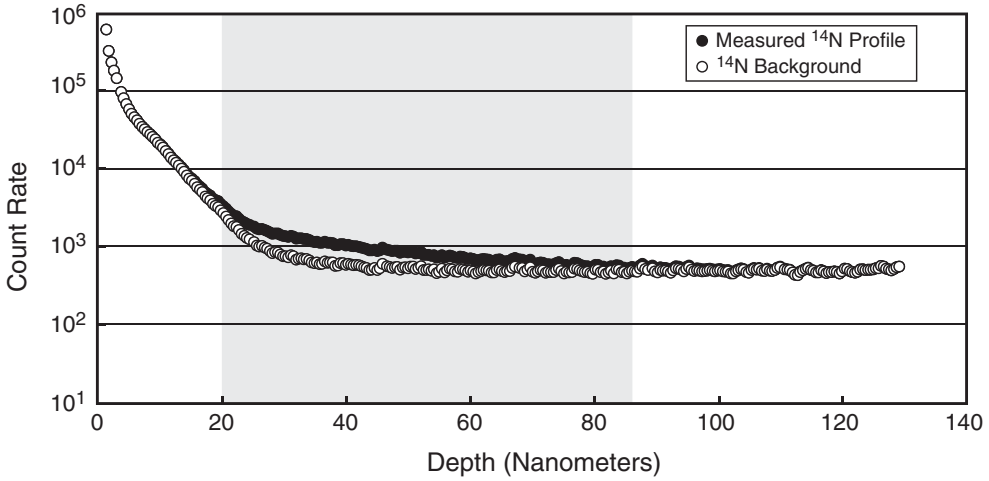

Fig. 4. An example of a measured ^{14}N profile in the B/C array (solid symbols) and the ^{14}N background (open symbols) calculated by subtracting the amount of solar wind profile (Fig. 1) required to make the background flat below approximately 40 nm. The steeply declining curve at shallow depths is a knock-on component of the adsorbed surface nitrogen. Although a vast majority of the surface nitrogen was removed by pumping and low-energy sputtering, the residual surface nitrogen causes significant problems with these measurements. The flat portion of the background profile is dominated by the nitrogen incorporated into the diamond-like carbon during manufacture. In data-reduction Method 2, the portion of the scaled SRIM profiles between 20 and 85 nm (the difference between the two curves in the shaded region) was used to calculate the nitrogen isotopic composition in the solar wind.

Table 1. $^{15}N/^{14}N$, $\delta^{15}N$[a], and nitrogen fluence from 9 measurements in Genesis B/C array fragment, 60628 (diamond-like-carbon collector film supported by a silicon substrate).

Measurement number	Background subtraction (Method 1)		SRIM modeling (Method 2)		Nitrogen fluence (atoms cm^{-2})
	$^{15}N/^{14}N$	$\delta^{15}N$	$^{15}N/^{14}N$	$\delta^{15}N$	
1[b]	0.00232	−368	0.00183	−502	2.36×10^{12}
2[b]	0.00208	−435	0.00209	−432	2.61×10^{12}
3	0.00223	−394	0.00193	−474	2.61×10^{12}
4	0.00270	−265	0.00239	−350	2.71×10^{12}
5	0.00208	−433	0.00223	−393	2.72×10^{12}
6	0.00177	−520	0.00204	−446	2.38×10^{12}
7	0.00225	−389	0.00204	−445	2.57×10^{12}
9	0.00237	−356	0.00245	−333	2.63×10^{12}
11	0.00174	−526	0.00206	−439	2.58×10^{12}
Average ± 2σ[c]	0.00217 ± 0.00037	−410 ± 100	0.00212 ± 0.00034	−424 ± 91	$(2.57 \pm 0.42) \times 10^{12}$

[a]Delta ^{15}N values calculated relative to a terrestrial $^{15}N/^{14}N$ value of 0.003676.
[b]First two measurements were made with 60 min of low-energy presputtering compared to 15 min for the other measurements.
[c]Uncertainties calculated as described in the Uncertainties and Determination of the 14N Fluence sections.
Measurement 8 was not used because magnetic field position was lost during the run.
Measurement 10 was not used because liquid nitrogen trap warmed up during the run.

standard deviations of the individual measurements in both cases. Thus, on statistical grounds, we would be justified in reporting the standard error of the sets of nine measurements as the uncertainty on the mean of the individual determination. But there are a number of nonstatistical uncertainties that must be considered. These include the uncertainty in the isotopic ratio used for the background correction and an uncertainty introduced from estimating the depth of the presputter crater. These can be quantified reasonably well by varying each parameter over the range of reasonable values that it can take and recording the effect on the final result. These uncertainties are independent, random, and are approximately normally distributed. Thus, they can be quadratically combined with the standard error to give an overall uncertainty. Uncertainties in the shape and depth of the calculated SRIM profiles are not easily quantified. There is also the uncertainty introduced by not making an instrumental mass-fractionation correction. Although this uncertainty is not random, it is independent and is the smallest of the quantified uncertainties. The uncertainties in the final

ratios reported for Method 1 and Method 2 in Table 1 are the quadratic combination of the standard error of the nine measurements, the uncertainty in the background correction, the uncertainty introduced from the estimated depth of the presputter crater, and the error due to the lack of a mass-fractionation correction.

Determination of the ^{14}N Fluence

To determine the nitrogen fluence, we used the scaled SRIM profiles from Method 2 described above for determining the $^{15}N/^{14}N$ ratio in the solar wind. The scaled profiles for the nine nitrogen measurements of the B/C array DOS collector were integrated numerically to give the total number of counts in each profile. The total counts in each profile were converted into a nitrogen fluence using a sensitivity factor calculated from the mean of three integrated depth profiles through our standard ^{15}N implant into DOS. The nominal implant level for ^{15}N was 1×10^{15} cm^{-2} (see above). The two-sigma uncertainty in the nitrogen fluence includes the standard error for the nine independent B/C-array measurements and a 16% uncertainty in the sensitivity factor.

RESULTS

Nitrogen Isotopic Composition

The $^{15}N/^{14}N$ ratios for the solar wind derived from the two methods described above are given in Table 1, both as ratios and as delta values relative to Earth's atmosphere. Two of the eleven measurements could not be used, one because the magnetic field centering lost the peaks in the middle of the run and one because the nitrogen trap warmed up in the middle of the run, generating a large background nitrogen signal. Table 1 also shows the means of the results from each of the two methods and our best estimate of the uncertainties in those numbers. The resulting values for $^{15}N/^{14}N$ in the solar wind from the two methods agree remarkably well ($[2.17 \pm 0.37] \times 10^{-3}$, $\delta^{15}N = -410 \pm 100‰$ and $[2.12 \pm 0.34] \times 10^{-3}$, $\delta^{15}N = -424 \pm 91‰$, errors are 2σ). Our results agree well with the value obtained by Marty et al. (2010) using laser extraction from the concentrator target holder gold cross ($[2.26 \pm 0.67] \times 10^{-3}$, $\delta^{15}N = -385 \pm 182‰$) and the more precise results of Marty et al. (2011) obtained by ion microprobe on the SiC concentrator target ($[2.18 \pm 0.02] \times 10^{-3}$, $\delta^{15}N = -407 \pm 7‰$).

Nitrogen Fluence

Table 1 summarizes our nitrogen fluence data. Our best estimate of the nitrogen fluence determined in the Genesis B/C DOS array is $(2.57 \pm 0.42) \times 10^{12}$ atoms per cm^2. The uncertainty in our final value is the quadratic combination of the standard error for the nine measurements and a 16% uncertainty in the sensitivity factor, derived from the reproducibility of the standards and an estimate of the uncertainty in the fluence of the standard implant. Our value is higher than that determined independently by "backside depth profiling" of a Genesis silicon collector ($[1.2 \pm 0.2] \times 10^{12}$ cm^{-2}; Heber et al. 2011a). While the largest absolute uncertainty may come from the uncertainty in the fluence of the standard implant, both Heber et al. (2011a) and this study used the same implant standard, so the difference between the two results cannot be assigned to the standard. Once a reliable value for the hydrogen fluence in the solar wind has been obtained for the Genesis collectors, fluence data for other elements such as nitrogen can be used to evaluate the metallicity of the Sun.

DISCUSSION

It was always clear that, as long as the fractionation introduced by the concentrator could be accounted for, more precise values of $^{15}N/^{14}N$ could be obtained by the analysis of concentrator targets. Knowing the solar nitrogen isotopic composition is important and was the number-2 priority objective of the Genesis mission. Consequently, the importance of the much more difficult measurements on collector array materials that we undertook was to show conclusively, as we have done, that the serious discrepancy between the results of Pepin et al. (2009) and the several measurements of concentrator targets was not due to some fundamental misunderstanding of the amounts of concentrator-induced isotopic fractionation. The ability to recognize and correct for anomalous results is a major advantage of sample return missions where replicate measurements by different techniques and/or laboratories can be made.

The $^{15}N/^{14}N$ ratio of the solar wind estimated from the measurements reported in this paper is approximately $(2.15 \pm 0.35) \times 10^{-3}$ ($\delta^{15}N \approx -417 \pm 100‰$ relative to the Earth's atmosphere). Although the uncertainty is relatively large, there is no doubt that our measurement shows the solar wind to be depleted in ^{15}N relative to the Earth's atmosphere, supporting the Nancy and UCLA results.

Marty et al. (2010) present a detailed discussion of the implications of the ^{14}N-rich composition for the solar wind. We do not review that discussion here, but attempt to extend portions of it. The isotopic fractionation of nitrogen due to inefficient Coulomb drag during acceleration of the solar wind is expected to be less than 5% favoring the light isotopes relative to the solar

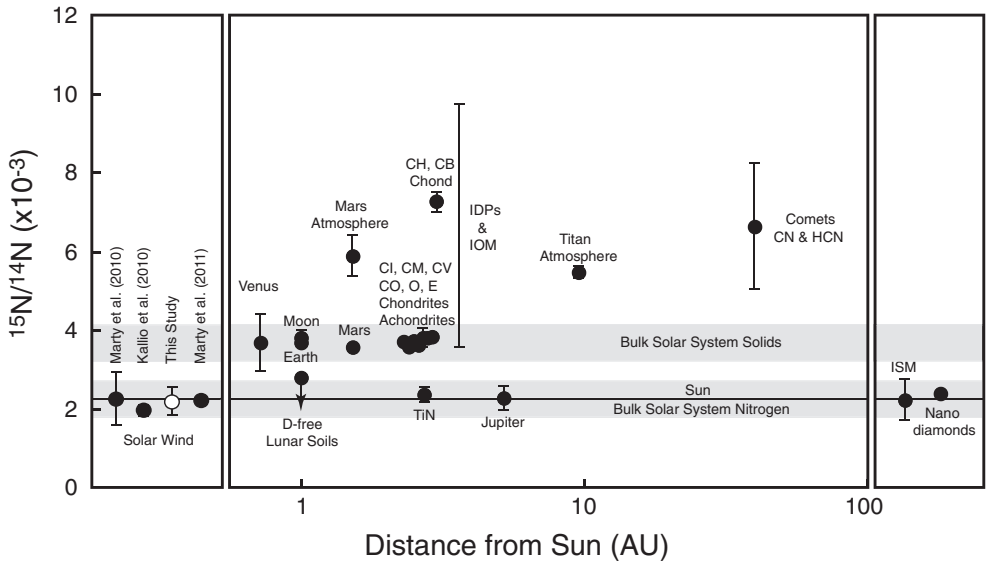

Fig. 5. Nitrogen isotopic ratios of various objects within and around our solar system are compared with the composition determined for the solar wind by this study, by Marty et al. (2010, 2011), and by Kallio et al. (2010). The solid line passing through the solar wind values, TiN, Jupiter, the ISM, and nanodiamonds gives the composition for the Sun determined by Marty et al. (2011) from their solar wind measurements. The lower shaded area gives the likely composition of the bulk solar system, which is dominated by the Sun. The upper shaded area is the region occupied by most solar system solids. The relationships between the plotted nitrogen compositions are discussed in the text. Data from Hoffman et al. (1979), Kerridge (1993), Dahmen et al. (1995), Russell et al. (1996), Lodders and Fegley (1998 and references therein), Hashizume et al. (2000), Owen et al. (2001), Mathew and Marti (2001), Abbas et al. (2004), Niemann et al. (2005), Meibom et al. (2007), Bockelée-Morvan et al. (2008), and Bonal et al. (2010).

convective zone (e.g., Bochsler 2007). The data for the solar wind presented in this study are not corrected for this effect, but this small fractionation is not significant for the discussion to follow. The composition for the Sun calculated by Marty et al. (2011) based on their precise solar wind measurement (plotted in Fig. 5) has been corrected for fractionation taking place in the convective zone of the sun (i.e., gravitational settling) and during acceleration of the solar wind.

Figure 5 shows various nitrogen reservoirs inside and outside of the solar system. The composition of the Sun, as inferred from measurements of the solar wind by this study and by Marty et al. (2010, 2011) and Kallio et al. (2010), lies at the ^{15}N-depleted end of the range of observed compositions. The nitrogen isotopic composition of solar wind in deuterium-free lunar soils also points to a similar composition (Hashizume et al. 2000). The Sun's nitrogen isotopic composition is thus similar to the composition measured in Jupiter's atmosphere (Owen et al. 2001; Abbas et al. 2004), in TiN from a primitive meteorite (Meibom et al. 2007), in meteoritic nanodiamonds (Russell et al. 1996), and in the local interstellar medium (Dahmen et al. 1995). The similarity in the compositions of the Sun and Jupiter implies that both acquired isotopically representative samples of bulk solar system nitrogen. The Sun's nitrogen composition also supports the suggestion that the TiN described by Meibom et al. (2007) condensed from a gas of solar composition. The agreement between the compositions of the Sun and the local interstellar medium indicates that the solar system is not anomalous relative to its surroundings. The close similarity between the composition of the Sun and that of nanodiamonds means that it is not possible to distinguish between a solar system and a presolar origin for the diamonds based on nitrogen. There are two viable models (1) the diamonds originated from a variety of sites throughout the galaxy, thus acquiring an average nitrogen composition of the interstellar medium; or (2) the majority of the nanodiamonds originated within the solar system from average solar system material.

All other solar system reservoirs have isotopically heavier nitrogen (Fig. 5). Venus, Earth, Mars' interior, and most chondrites and achondrites exhibit a small range of nitrogen isotopic compositions, all of which are significantly enriched in ^{15}N relative to the composition of the Sun (Hoffman et al. 1979; Lodders and Fegley 1998; Mathew and Marti [2001] and references therein). The interior of the Moon also may have nitrogen of a similar composition (e.g., Kerridge 1993). In some ways, the situation for nitrogen is analogous to that for oxygen, where solar oxygen is ^{16}O-rich (isotopically light) compared with the Earth and most other inner solar system materials (McKeegan et al. 2011). Venus, Earth,

and Mars are differentiated bodies, while chondrites have had a much less extensive postaccretional history. This implies that the nitrogen compositions of these objects are not the result of a variety of different mass-dependent fractionation events in the histories of the various bodies operating on a solar composition. Apparently, the materials that accreted to form the terrestrial planets and meteorites were already enriched in ^{15}N relative to the solar composition; i.e., these materials became ^{15}N-rich prior to the formation of all of these bodies.

Large-scale mechanisms that could generate global ^{15}N enrichments in condensed phases are not well understood. N_2 self-shielding is one potential mechanism (e.g., Lyons 2009, 2010). This is analogous to the self-shielding of oxygen that has been proposed as the dominant mechanism for mass-independent oxygen isotopic fractionation in the solar system (e.g., Clayton 2002). However, while it is possible to model moderate nitrogen isotopic fractionations in the gas phase under plausible nebula conditions, it is not clear how ^{15}N enrichments can be preserved in the solids (e.g., Lyons 2009; Lyons et al. 2009). Ion-molecule reactions, either in the Sun's parent molecular cloud or in the cold outer solar system, also could potentially produce widespread enrichments of ^{15}N in solids. Rodgers and Charnley (2008) demonstrated that enrichments of up to a factor of several in ^{15}N relative to the starting composition can occur in NH_3 ice. However, it is not clear how these enrichments would have been trapped in the solid materials that became the terrestrial planets and meteorite parent bodies. It is probable that the combination of processes that affected gas and dust in interstellar space and in the early solar system tend to fractionate nitrogen such that the solids are enriched in ^{15}N, and this combination of processes is responsible for the isotopic offset between the Sun and the rocky bodies. Considerable work will be required to understand how this works, both for nitrogen and for oxygen.

A variety of materials are more enriched in ^{15}N than the majority of rocky bodies, including the Mars atmosphere, CB/CH chondrites, organic materials within primitive chondrites and IDPs, comets, and Titan's atmosphere. These additional enrichments of ^{15}N most likely reflect processes specific to each of these reservoirs. For example, the high $^{15}N/^{14}N$ ratio in the Mars atmosphere can be understood as reflecting preferential loss of ^{14}N during nonthermal escape from the top of the atmosphere (Fox and Dalgarno 1983). The same appears to be true for the atmosphere of Titan (Lammer et al. 2000; Niemann et al. 2005).

The organic material in chondrites and IDPs contains tiny grains that are highly enriched in ^{15}N, and the organic material itself is, on average, more ^{15}N rich than the nitrogen on Earth (e.g., Alexander et al. 2007). Figure 5 was created to illustrate the range of nitrogen isotopic compositions in solar system bodies. The figure does not contain any information about the relative abundances of the various compositions. Most of the organic materials are somewhat enriched relative to the Earth, but only a small fraction is extremely enriched. Some of the ^{15}N-rich components may have a nucleosynthetic origin, but for most, other origins are indicated. Large nitrogen isotopic fractionation can potentially be recorded in amine and nitrile functional groups incorporated into refractory organic material on grain surfaces in interstellar clouds (Rodgers and Charnley 2008). This organic material is one of the components that went into the rocky bodies of the early solar system, but its relatively extreme composition was probably diluted by other nitrogen components in bulk objects. The relative abundances of organic materials and other components are relatively similar in fine-grained materials in primitive chondrites (e.g., Huss et al. 2003), so the mixing ratios of various components in the rocky bodies were probably similar, giving a similar bulk nitrogen composition to the various objects.

The CH and CB chondrites (Fig. 5) are a special case. These chondrites formed relatively late during solar system formation and have had a strange history (e.g., Krot et al. 2005). Some of the components may have formed via an impact between planetary embryos (Krot et al. [2005] and references therein). The CH and CB chondrites have the highest bulk $^{15}N/^{14}N$ ratios among chondritic meteorites ($^{15}N/^{14}N \approx 7.3 \times 10^{-3}$; $\delta^{15}N \approx +1000‰$) (e.g., Prombo and Clayton 1985; Ivanova et al. 2008). Dark inclusions within the Isheyevo CH/CB have very high $^{15}N/^{14}N$ ratios, even higher than the bulk meteorites (Bonal et al. 2010). In contrast, the TiN-bearing CAI, which has solar-Jupiter-like nitrogen isotopic composition (Meibom et al. 2007), is also from Isheyevo. Thus, while the origin of the ^{15}N enrichments is not at all clear, it is apparently unique to non-CAI components of CH and CB chondrites and likely results from several stages of nitrogen isotopic fractionation.

The nitrogen isotopic compositions for comets (Fig. 5) come from measurements of CN and HCN coma molecules (e.g., Bockelée-Morvan et al. 2008). If these compounds are representative of bulk comets, then the material that accreted to form comets underwent nitrogen isotopic fractionation either prior to or during accretion. However, these compounds may reflect molecular-cloud or outer-solar-system chemistry that is specific to the HCN molecule (Rodgers and Charnley 2008) and thus may not be representative of either the bulk comets, where nitrogen is also sited in other compounds, or of the outer solar nebula as a whole.

In summary, the isotopic composition of the Sun, and by extension the bulk solar system, is depleted in

^{15}N relative to essentially all solar system solids. The relative enrichments of ^{15}N in the solids may reflect two sequential stages of nitrogen isotopic fractionation: (1) an early stage that produced a global fractionation in the solid materials that became the meteorites and the terrestrial planets, and (2) a second stage that further fractionated the nitrogen in some reservoirs, such as the atmospheres of Mars and Titan and the CH/CB chondrites. Some objects, such as comets and IDPs, may preserve a record of some of the processes that generated the global fractionation in solid materials.

CONCLUSIONS

We have measured the isotopic composition and fluence of nitrogen in diamond-like carbon flown on the Genesis B/C array. We found a $^{15}N/^{14}N$ ratio for the solar wind of approximately $(2.15 \pm 0.35) \times 10^{-3}$ ($\delta^{15}N \approx -417 \pm 100‰$ relative to the Earth's atmosphere), consistent with results of Marty et al. (2010, 2011) and Kallio et al. (2010) and distinctly different from the ^{15}N-enriched composition found by Pepin et al. (2009). The measured nitrogen composition of the solar wind is expected to be very close to the composition of the Sun and is quite similar to the compositions of Jupiter, TiN thought to have condensed from the solar nebula, meteoritic nanodiamonds, and the interstellar medium. All other solar system materials have higher $^{15}N/^{14}N$ ratios. The distribution of these compositions suggests that they represent two stages of nitrogen fractionation: (1) a global fractionation that systematically increased the $^{15}N/^{14}N$ ratio of the materials that became the rocky bodies in the solar system relative to the bulk solar system and the Sun, and (2) additional mass-dependent fractionations associated specifically with the formation of individual objects. Observations of comets and the gases in their comas and isotopic data for organic materials in IDPs and extracted from meteorites may provide clues to the global processes that enriched the nitrogen in the solids in ^{15}N.

Our nitrogen fluence measurement ($[2.57 \pm 0.42] \times 10^{12}$ cm^{-2}) is higher than that obtained by Heber et al. (2011a) from backside profiling of a silicon collector. Reliable fluence measurements for hydrogen, nitrogen, and several other elements in the Genesis collectors will help evaluate the metallicity of the Sun.

Acknowledgments—This paper benefited from helpful reviews by Veronika Heber, Andrew Davis, and Bernard Marty. It was supported by NASA grant NNX09AC32G to GRH and NNX09AC35G to DSB. This is Hawai'i Institute of Geophysics and Planetology publication No. 1977 and School of Ocean and Earth Science and Technology publication No. 8696. Los Alamos National Laboratory publication LA-UR-12-24206.

Editorial Handling—Dr. Ian Franchi

REFERENCES

Abbas M. M., LeClair A., Owen T., Conrath B. J., Flasar F. M., Kunde V. G., Nixon C. A., Achterberg R. K., Bjoraker G., Jennings D. J., Orton G., and Romani P. N. 2004. The nitrogen isotopic ratio in Jupiter's atmosphere from observations by the composite infrared spectrometer on the *CASSINI* spacecraft. *The Astrophysical Journal* 602:1063–1074.

Alexander C. M. O'D., Fogel M., Yabuta H., and Cody G. D. 2007. The origin and evolution of chondrites recorded in the elemental and isotopic compositions of their macromolecular organic matter. *Geochimica et Cosmochimica Acta* 71:4380–4403.

Becker R. H. 2010. Solar wind $^{15}N/^{14}N$ from Genesis—A tale of two values (abstract #2469). 41st Lunar and Planetary Science Conference. CD-ROM.

Bochsler P. 2007. Minor ions in the solar wind. *Astronomy & Astrophysics Reviews* 14:1–40.

Bockelée-Morvan D., Biver N., Jehin E., Cochran A. L., Wiesemeyer H., Manfroid J., Hutsemékers D., Arpigny C., Boissier J., Cochran W., Colom P., Crovisier J., Milutinovic N., Moreno R., Prochaska J. X., Ramirez I., Schulz R., and Zucconi J.-M. 2008. Large excess of heavy nitrogen in both hydrogen cyanide and cyanogens from comet 17P/Holmes. *The Astrophysical Journal* 679:L49–L52.

Bodmer R. and Bochsler P. 2000. Influence of Coulomb collisions on isotopic and elemental fractionation in the solar wind acceleration process. *Journal of Geophysical Research* 105:47–60.

Bonal L., Huss G. R., Krot A. N., Nagashima K., Ishii H. A., and Bradley J. P. 2010. Highly ^{15}N-enriched chondritic clasts in the CB/CH-like meteorite Isheyevo. *Geochimica et Cosmochimica Acta* 74:6590–6609.

Burnett D. S., Barraclough B. L., Bennett R., Neugebauer M., Oldham L. P., Sasaki C. N., Sevilla D., Smith N., Stansbery E., Sweetnam D., and Wiens R. C. 2003. The Genesis discovery mission: Return of solar matter to Earth. *Space Science Reviews* 105:509–534.

Clayton R. N. 2002. Self-shielding in the solar nebula. *Nature* 415:860–861.

Dahmen G., Wilson T. L., and Matteucci F. 1995. The nitrogen isotope abundance in the galaxy. *Astronomy & Astrophysics* 295:194–198.

Fox J. L. and Dalgarno A. 1983. Nitrogen escape from Mars. *Journal of Geophysical Research* 88:9027–9032.

Geiss J. and Bochsler P. 1982. Nitrogen isotopes in the solar system. *Geochimica et Cosmochimica Acta* 46:529–548.

Geiss J. and Bochsler P. 1991. Long time variations in solar wind properties: Possible causes versus observations. In *The sun in time*, edited by Sonett C. P., Giampapa M. S., Matthews M. S., and Mitton J. Tucson, AZ: The University of Arizona Press. pp. 98–117.

Geiss J., Gloeckler G., and von Steiger R. 1994. Solar and heliospheric processes from solar wind composition measurements. *Philosophical Transactions of the Royal Society of London, Series A* 349:213–226.

Hashizume K., Chaussidon M., Marty B., and Robert F. 2000. Solar wind record on the Moon: Deciphering presolar from planetary nitrogen. *Science* 290:1142–1145.

Heber V. S., Guan Y., Jurewicz A. J. G., Smith S., Olinger C., McKeegan K. D., and Burnett D. S. 2011a. Abundances of carbon, nitrogen and oxygen in the solar wind measured by

backside SIMS depth profiling (abstract #2642). 42nd Lunar and Planetary Science Conference. CD-ROM.

Heber V. S., Wiens R. C., Jurewicz A. J. G., Vogel N., Reisenfeld D. B., Baur H., McKeegan K. D., Wieler R., and Burnett D. S. 2011b. Isotopic and elemental fractionation of solar wind implanted in the Genesis concentrator target characterized and quantified by noble gases. *Meteoritics & Planetary Science* 46:493–512.

Hoffman J. H., Hodges R. R., Jr., McElroy M. B., Donahue T. M., and Kolpin M. 1979. Composition and structure of Venus Atmosphere. *Science* 205:49–52.

Huss G. R., Meshik A. P., Smith J. B., and Hohenberg C. M. 2003. Presolar diamond, silicon carbide, and graphite in carbonaceous chondrites: Implications for thermal processing in the solar nebula. *Geochimica et Cosmochimica Acta* 67:4823–4848.

Ivanova M. A., Kononkova N. N., Krot A. N., Greenwood R. C., Franchi I. A., Verchovsky A. B., Trieloff M., Korochantseva E. V., and Brandstaetter F. 2008. The Isheyevo meteorite: Mineralogy, petrology, bulk chemistry, oxygen, nitrogen, and carbon isotopic composition and ^{40}Ar-^{39}Ar ages. *Meteoritics & Planetary Science* 43:915–940.

Jurewicz A. J. G., Burnett D. S., Wiens R. C., Friedmann T. A., Hays C. C., Hohlfelder R. J., Nishiizumi K., Stone J. A., Woolum D. S., Becker R., Butterworth A. L., Campbell A. J., Ebihara M., Franchi I. A., Heber V., Hohenberg C. M., Humayun M., McKeegan K. D., McNamara K., Meshik A., Pepin R. O., Schlutter D., and Wieler R. 2003. The Genesis solar-wind collector materials. *Space Science Reviews* 105:535–560.

Kallio A. P. A., McKeegan K. D., Jarzebinski G., Mao P. H., Kunihiro T., Coath C. D., Heber V. S., Burnett D. S., and Wiens R. C. 2010. Nitrogen isotopic composition of solar wind returned by the Genesis mission (abstract #2481). 41st Lunar and Planetary Science Conference. CD-ROM.

Kerridge J. F. 1993. Long-term compositional variation in solar corpuscular radiation—Evidence from nitrogen isotopes in the lunar regolith. *Reviews of Geophysics* 31:423–437.

Kim J. S., Kim Y., Marti K., and Kerridge J. F. 1995. Nitrogen isotope abundances in the recent solar wind. *Nature* 375:383–385.

Krot A. N., Amelin Y., Cassen P., and Meibom A. 2005. Young chondrules in CB chondrites from a giant impact in the early solar system. *Nature* 436:989–992.

Lammer H., Stumptner W., Molina-Cuberos G. J., Bauer S. J., and Owen T. 2000. Nitrogen isotopic fractionation and its consequences for Titan's atmospheric evolution. *Planetary and Space Science* 48:529–543.

Lodders K. and Fegley B., Jr. 1998. *The planetary scientist's companion*. New York: Oxford University Press. 371 pp.

Lyons J. T. 2009. N_2 self-shielding in the solar nebula. *Meteoritics & Planetary Science* 44:A126.

Lyons J. R. 2010. N_2 self-shielding in the solar nebula: An update. *Meteoritics & Planetary Science* 45:A123.

Lyons J. R., Bergin E. A., Ciesla F. J., Davis A. M., Desch S. J., Hashizume K., and Lee J. E. 2009. Timescales for the evolution of oxygen isotope compositions in the solar nebula. *Geochimica et Cosmochimica Acta* 73:4998–5017.

Mao P. H., Burnett D. S., Coath C. D., Jarzebinski G., Kunihiro T., and McKeegan K. D. 2008. MegSIMS: A SIMS/AMS hybrid for measurement of the Sun's O isotopic composition. *Applied Surface Science* 255:1461–1464.

Marty B., Zimmermann L., Burnard P. G., Wieler R., Heber V. S., Burnett D. L., Wiens R. C., and Bochsler P. 2010. Nitrogen isotopes in the recent solar wind from the analysis of Genesis targets: Evidence for large scale isotope heterogeneity in the early solar system. *Geochimica et Cosmochimica Acta* 74:340–355.

Marty B., Chaussidon M., Wiens R. C., Jurewicz A. J. G., and Burnett D. S. 2011. A ^{15}N-poor isotopic composition for the solar system as shown by Genesis solar wind samples. *Science* 332:1533–1536.

Mathew K. J. and Marti K. 2001. Early evolution of Martian volatiles: Nitrogen and noble gas components in ALH 84001 and Chassigny. *Journal of Geophysical Research* 106:1401–1422.

McKeegan K. D., Kallio A. P. A., Heber V. S., Jarzebinski G., Mao P. H., Coath C. D., Kunihiro T., Wiens R., Allton J., and Burnett D. S. 2010. Genesis SiC concentrator sample traverse: Confirmation of ^{16}O-depletion of terrestrial oxygen (abstract #2589). 41st Lunar and Planetary Science Conference. CD-ROM.

McKeegan K. D., Kallio A. P. A., Heber V. S., Jarzebinski G., Mao P. H., Coath C. D., Kunihiro T., Wiens R., Nordholt J. E., Moses R. W., Jr., Reisenfeld D. B., Jurewicz A. J. G., and Burnett D. S. 2011. The oxygen isotopic composition of the Sun inferred from captured solar wind. *Science* 332:1528–1532.

Meibom A., Krot A. N., Robert F., Mostefaoui S., Russell S. S., Petaev M. I., and Gounelle M. 2007. Nitrogen and carbon isotopic composition of the Sun inferred from a high-temperature solar nebular condensate. *The Astrophysical Journal* 656:L33–L36.

Niemann H. B., Atreya S. K., Bauer S. J., Carignan G. R., Demick J. E., Frost R. L., Gautier D., Haberman J. A., Harpold D. N., Hunten D. M., Israel G., Lunine J. I., Kasprzak W. T., Owen T. C., Paulkovich M., Raulin F., Raaen E., and Way S. H. 2005. The abundances of constituents of Titan's atmosphere from the GCMS instrument on the Huygens probe. *Nature* 438: 779–784.

Owen T., Mahaffy P. R., Niemann H. B., Atreya S., and Wong M. 2001. Protosolar nitrogen. *The Astrophysical Journal* 553:L77–L79.

Pepin R. O., Becker R. H., and Schlutter D. J. 2009. Solar wind nitrogen in Genesis gold-on-sapphire (AuOS) collectors (abstract #2103). 40th Lunar and Planetary Science Conference. CD-ROM.

Prombo C. and Clayton R. N. 1985. A striking nitrogen isotope anomaly in the Bencubbin and Weatherford meteorites. *Science* 230:935–937.

Rodgers S. D. and Charnley S. B. 2008. Nitrogen isotopic fractionation of interstellar nitriles. *The Astrophysical Journal* 689:1448–1455.

Russell S. S., Arden J. W., and Pillinger C. T. 1996. A carbon and nitrogen isotopic study of diamond from primitive chondrites. *Meteoritics and Planetary Science* 31: 343–355.

von Steiger R., Schwadron N. A., Fisk L. A., Geiss J., Gloeckler G., Hefti S., Wilken B., Wimmer-Schweingruber R. F., and Zurbuchen T. H. 2000. Composition of quasi-stationary solar wind flows from Ulysses/Solar Wind Ion Composition Spectrometer. *Journal of Geophysical Research* 105:27,217–27,238.

Wieler R., Humbert F., and Marty B. 1999. Evidence for a predominantly non-solar origin of nitrogen in the lunar

regolith revealed by single grain analyses. *Earth and Planetary Science Letters* 167:47–60.

Wiens R. C., Neugebauer M., Reisenfeld D. B., Moses R. W., Jr., Nordholt J. E., and Burnett D. S. 2003. Genesis solar wind concentrator: Computer simulations of performance under solar wind conditions. *Space Science Reviews* 105:601–625.

Ziegler J. F. 2004. SRIM-2003. *Nuclear Instruments and Methods in Physics Research B* 219–220:1027–1036.

Ziegler J. F., Ziegler M. D., and Biersack J. P. 2010. SRIM—The stopping and range of ions in matter (2010). *Nuclear Instruments and Methods in Physics Research B* 268:1818–1823.